

# Emission of neutron-proton and proton-proton pairs in neutrino scattering

I. Ruiz Simo<sup>a</sup>, J.E. Amaro<sup>a</sup>, M.B. Barbaro<sup>b,c</sup>, A. De Pace<sup>c</sup>, J.A. Caballero<sup>d</sup>, G.D. Megias<sup>d</sup>, T.W. Donnelly<sup>e</sup>

<sup>a</sup>*Departamento de Física Atómica, Molecular y Nuclear,*

*and Instituto de Física Teórica y Computacional Carlos I, Universidad de Granada, Granada 18071, Spain*

<sup>b</sup>*Dipartimento di Fisica, Università di Torino, Via P. Giuria 1, 10125 Torino, Italy*

<sup>c</sup>*INFN, Sezione di Torino, Via P. Giuria 1, 10125 Torino, Italy*

<sup>d</sup>*Departamento de Física Atómica, Molecular y Nuclear,*

*Universidad de Sevilla, Apdo.1065, 41080 Sevilla, Spain and*

<sup>e</sup>*Center for Theoretical Physics, Laboratory for Nuclear Science and Department of Physics, Massachusetts Institute of Technology, Cambridge, MA 02139, USA*

(Dated: October 8, 2018)

We use a recently developed model of relativistic meson-exchange currents to compute the neutron-proton and proton-proton yields in  $(\nu_\mu, \mu^-)$  scattering from  $^{12}\text{C}$  in the 2p-2h channel. We compute the response functions and cross sections with the relativistic Fermi gas model for different kinematics from intermediate to high momentum transfers. We find a large contribution of neutron-proton configurations in the initial state, as compared to proton-proton pairs. In the case of charge-changing neutrino scattering the 2p-2h cross section of proton-proton emission (*i.e.*, np in the initial state) is much larger than for neutron-proton emission (*i.e.*, two neutrons in the initial state) by a  $(\omega, q)$ -dependent factor. The different emission probabilities of distinct species of nucleon pairs are produced in our model only by meson-exchange currents, mainly by the  $\Delta$  isobar current. We also analyze other effects including exchange contributions and the effect of the axial and vector currents.

PACS numbers: 25.30.Fj; 21.60.Cs; 24.10.Jv

## I. INTRODUCTION

The identification of nuclear effects in neutrino scattering is essential for modern neutrino oscillation experiments [1–7]. In particular the sensitivity of the neutrino energy reconstruction to multi-nucleon events has been stressed in recent data analyses [8]. In the MINERvA neutrino experiment an enhanced population of multi-proton states has been observed between the quasielastic and  $\Delta$  peaks. On the other hand, observation of events with a pair of energetic protons at the interaction vertex accompanying the muon in  $^{40}\text{Ar}(\nu_\mu, \mu^-)$  reaction has been reported in the ArgoNeuT experiment [9]. From these events several back-to-back nucleon configurations have been identified and associated with nuclear mechanisms involving short-range correlated (SRC) neutron-proton (np) pairs in the nucleus [10]. However in [11] these “hammer events” have been modeled by a simple pion production and reabsorption model without nucleon-nucleon correlations, suggesting that the distribution of pp pairs in the final state is less sensitive to details of the initial pair configuration. In the opinion of the authors of [11], the events cannot teach us anything significant about SRC. The NUWRO event generator supports that the excess of back-to-back events in ArgoNeuT has a kinematic origin and is not directly related to SRC [12].

SRC with back-to-back configurations have been also identified in two-nucleon knock-out electron scattering experiments on  $^{12}\text{C}$  for high momentum transfer and missing momentum [13, 14]. In this case one expects an excess of np pairs over pp pairs [15, 16]. The experiment reported a number of np pairs 18 times larger than

their pp counterparts. The analysis of these experiments is compatible with theoretical single-nucleon and nucleon pair momentum distributions in variational Monte Carlo calculations, where the importance of the tensor forces in the ground-state correlations of nuclei has been emphasized [17, 18]. While the kinematics of the experiments have been selected to minimize the contribution from other mechanisms that can induce two-particle emission, such as meson-exchange currents (MEC) and isobar excitations [13], the contribution of MEC cannot be ruled out *a priori* [19].

In this work we investigate the relative effect of MEC on the separate pp and np channels in the inclusive 2p-2h neutrino cross section. It has been emphasized that the separate charge distributions of 2p-2h events are useful. One of the reasons is for their use in Monte Carlo event generators [12, 20]. For instance in NUWRO configurations the MEC 2p-2h excitations are assumed to occur 95% of the time for events where the interaction occurs in initial np pairs [12, 21] (or final pp pairs for charged current neutrino scattering). This value was estimated based on the assumption, claimed also in [22], that neutrinos interact mostly with correlated np pairs. From a naive calculation this value agrees with a factor 18/19, corresponding to the extracted value of  $\text{np}/(\text{np}+\text{pp})$  in the  $^{12}\text{C}(e, e'Np)$  experiment of [13]. However this neutrino generator uses a 2p-2h model that does not give separate pp and np contributions, and therefore this choice is not fully consistent from the theoretical point of view [12]. On the other hand it is expected that the ratio between np and pp interactions should be kinematics dependent and not only a global factor. Thus a theoretical quantification of the np/pp ratio and its dependence on the

typical kinematics would be desired for each implementation of 2p-2h cross sections. Results for the separate pp and np contributions due to short-range correlations have been presented in [23], for the  $R_T$  and  $R_{CC}$  response functions, and for  $q = 400$  MeV/c, but not for the differential cross section. The contribution of initial np pairs to the T response found in [23] is about twice that of the initial nn pairs.

We have recently developed a fully relativistic model of meson-exchange currents in the 2p-2h channel for electron and neutrino scattering [24]. This model is an extension of the relativistic MEC model of [25] to the weak sector. It has been recently validated by comparing to the  $^{12}\text{C}(e, e')$  inclusive cross section data for a wide kinematic range within the SuperScaling approach (SuSA) [26]. This model describes jointly the quasielastic and inelastic regions using two scaling functions fitted to reproduce the data, while the 2p-2h MEC contribution properly fills the dip region in between, resulting in excellent global agreement with the data. The model has been recently extended to the description of neutrino scattering reactions for a variety of experiments providing an excellent agreement with data [27]. With this benchmark model we are able to study the separate np and pp channels in the response functions and cross section for the three  $(e, e')$ ,  $(\nu_l, l^-)$  and  $(\bar{\nu}_l, l^+)$  reactions. While this analysis was performed in [19] for electron scattering, in this work we consider neutrino reactions. Our model includes the contributions of pion-in-flight, seagull, pion-pole and  $\Delta(1232)$  excitation diagrams of the MEC. The two-body matrix elements between relativistic spinors were presented in our recent work [24], where they have been deduced from the weak pion production amplitudes of [28].

## II. FORMALISM FOR NEUTRINO SCATTERING

The formalism of 2p-2h cross section including MEC in the relativistic Fermi gas was given in [24]. We write the charged current (CC) cross section as

$$\frac{d\sigma}{d\Omega' d\epsilon'} = \sigma_0 \left[ \tilde{V}_{CC} R^{CC} + 2\tilde{V}_{CL} R^{CL} + \tilde{V}_{LL} R^{LL} + \tilde{V}_T R^T \pm 2\tilde{V}_{T'} R^{T'} \right], \quad (1)$$

where  $\sigma_0$  is a kinematic factor including the weak couplings defined in [29, 30]. Note that there is a linear combination of five response functions, labeled as  $CC, CL, LL, T$  and  $T'$ . The  $T'$  response function contributes differently for neutrinos (plus sign) than for antineutrinos (minus sign). The  $\tilde{V}_K$  factors are kinematic functions that were defined in [29, 30].

The response functions  $R^K(\omega, q)$  depend on the energy and momentum transfer. They are computed here in a relativistic Fermi gas (RFG) model, with Fermi momentum  $k_F$ , where they can be expanded as the sum of

one-particle one-hole (1p-1h), two-particle two-hole (2p-2h), plus additional channels. Here we are interested in the 2p-2h channel, where two nucleons with momenta  $\mathbf{p}'_1$  and  $\mathbf{p}'_2$  are ejected out of the Fermi sea,  $p'_i > k_F$ , leaving two hole states in the daughter nucleus, with momenta  $\mathbf{h}_1$  and  $\mathbf{h}_2$  (with  $h_i < k_F$ ).

The 2p-2h response functions are computed as

$$R_{2p-2h}^K = \frac{V}{(2\pi)^9} \int d^3p'_1 d^3h_1 d^3h_2 \frac{m_N^4}{E_1 E_2 E'_1 E'_2} r^K(\mathbf{p}'_1, \mathbf{p}'_2, \mathbf{h}_1, \mathbf{h}_2) \delta(E'_1 + E'_2 - E_1 - E_2 - \omega) \times \theta(p'_2 - k_F) \theta(p'_1 - k_F) \times \theta(k_F - h_1) \theta(k_F - h_2), \quad (2)$$

where the momentum of the second nucleon is fixed by momentum conservation inside the integral sign,  $\mathbf{p}'_2 = \mathbf{h}_1 + \mathbf{h}_2 + \mathbf{q} - \mathbf{p}'_1$ ,  $V$  is the volume of the system,  $m_N$  is the nucleon mass, while  $E_i$  and  $E'_i$  are the energies of the holes and particles, respectively.

Using energy conservation, the calculation of the inclusive 2p-2h responses of Eq. (2) for given energy and momentum transfer  $(\omega, q)$ , is reduced to a seven-dimensional integral that is computed numerically following the methods developed in [31, 32]. The main ingredient of the calculation is the set of five response functions  $r^K(\mathbf{p}'_1, \mathbf{p}'_2, \mathbf{h}_1, \mathbf{h}_2)$ , for the elementary 2p-2h transition. These elementary response functions are written in terms of the two-body MEC antisymmetrized matrix elements, summed over spin. We separate the contributions of the different charge channels to the response functions. These can be  $(np, pp)$  for neutrinos, and  $(np, nn)$  for antineutrinos. In [24] we derived general formulae for the separate np and pp response functions.

The total CC MEC for neutrino scattering can be written as

$$j_{\text{MEC}}^\mu = \tau_+(1) J_1^\mu(1' 2'; 1 2) + \tau_+(2) J_2^\mu(1' 2'; 1 2) + (I_V)_+ J_3^\mu(1' 2'; 1 2), \quad (3)$$

where  $\tau_+ = \tau_x + i\tau_y$  and we have defined the isospin operators

$$(I_V)_\pm = (I_V)_x \pm i(I_V)_y \quad (4)$$

that stands for the  $\pm$ -component of the two-body isovector operator

$$\mathbf{I}_V = i[\boldsymbol{\tau}(1) \times \boldsymbol{\tau}(2)]. \quad (5)$$

The isospin-independent two-body currents  $J_1^\mu$ ,  $J_2^\mu$ , and  $J_3^\mu$ , follow from the amplitudes of weak pion production model of [28] and are written in [24].

In other models of neutrino scattering [22, 33], only the direct diagrams (a,b) of Fig. 1 are included, while the direct-exchange contribution corresponding to the diagrams (c,d) are disregarded. In our model, on the contrary, both contributions are considered. The elementary

2p-2h transverse response function is given for pp emission by

$$r_{pp}^T = 4 \sum_{\mu=1}^2 \sum_{s_1 s_2 s'_1 s'_2} \left\{ |J_{pp}^\mu(1'2'; 12)|^2 - \text{Re } J_{pp}^\mu(1'2'; 12)^* J_{pp}^\mu(2'1'; 12) \right\}, \quad (6)$$

where  $J_{pp}^\mu(1'2'; 12)$  is the effective two-body current for pp emission with neutrinos given by

$$J_{pp}^\mu = J_1^\mu + J_3^\mu. \quad (7)$$

The first term in the transverse response is the “direct” contribution, and the second one is the “exchange” contribution, actually being the interference between the direct and exchange matrix elements.

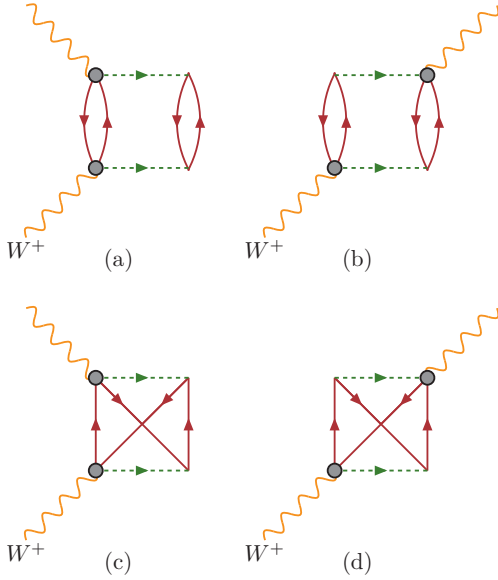


FIG. 1: (Color online) Some contributions of 2p-2h states to the response functions considered in this work. The circle stands for the elementary  $W^+N \rightarrow \pi N$  amplitude. Diagrams (a,b) represent the direct contribution. Diagrams (c,d) are the exchange contributions.

The elementary transverse response for np emission has a similar expression

$$r_{np}^T = 4 \sum_{\mu=1}^2 \sum_{s_1 s_2 s'_1 s'_2} \left\{ |J_{np}^\mu(1'2'; 12)|^2 - \text{Re } J_{np}^\mu(1'2'; 12)^* J_{np}^\mu(1'2'; 21) \right\}, \quad (8)$$

but with the effective current  $J_{np}^\mu$  for np emission

$$J_{np}^\mu = J_2^\mu + J_3^\mu, \quad (9)$$

which is in general different from the pp one because of the distinct isospin matrix elements. The direct contribution corresponds to neglecting the second terms in Eqs. (6,8).

### III. RESULTS

In the following we present results for the semi-inclusive  $^{12}\text{C}(\nu_\mu, \mu^- pp)$  and  $^{12}\text{C}(\nu_\mu, \mu^- np)$  reactions, corresponding to the 2p-2h channel of the  $^{12}\text{C}(\nu_\mu, \mu^-)$  reaction in the two separate charge channels in the final hadronic state corresponding to two-nucleon knockout. Our MEC model and its parameters were obtained from the pion production amplitudes of [28]. This is an extension of the electromagnetic MEC model of [25] to the weak sector.

The five MEC-induced 2p-2h responses for CC neutrino interactions at fixed momentum transfer are shown in Fig. 2. The Coulomb  $R_{CC}$  and transverse  $R_T$  responses are also present in electron scattering. In general the  $\omega$  dependence of the 2p-2h responses shows a broad peak coming from the  $\Delta$  excitation. The strength of the MEC peak weakens with  $q$  due to the decrease of the electroweak form factor with  $Q^2$ , especially the  $\Delta$  form factors. Note also that the most important contribution to the neutrino cross section comes from the two transverse responses  $R_T$  and  $R_{T'}$ . In the figure we only show the separate pp and np 2p-2h response functions, the total responses being the sum of the two. For all the cases in Fig. 2 we observe that the pp response functions are much larger than the np ones by a factor 6 or less depending on the kinematics.

The pp/np ratio in the present neutrino calculation can be compared to the np/pp ratio in the  $(e, e')$  reaction studied in [19], because they correspond to the same pairs in the initial state. For the transverse response that ratio for neutrino scattering is roughly a factor of two smaller than for the electron case.

For  $q = 400 \text{ MeV}/c$  our results for  $R_T$  can be compared to those of the SRC model of [23]. Our MEC response at the maximum is one order of magnitude larger than that of the SRC one. In our calculation, the pp pair emission transverse response induced by MEC is about a factor of 6 larger than the np one. In contrast, the mentioned SRC model shows at most a factor of 3 between the two contributions. The order of magnitude of the  $R_{CC}$ , on the other hand, is small in both MEC and SRC 2p-2h responses, but still the MEC results are about twice those of [23]. The pp pairs in the final state continue to dominate the  $R_{CC}$  MEC response, while in the SRC case, both pairs contribute similarly.

Although the behaviors of MEC and SRC 2p-2h responses are completely different, one should emphasize that the cross section is dominated by the transverse responses. One could conclude from this comparison that the MEC are the largest contribution to the 2N knockout strength, and that the influence of SRC is around 10%.

In a previous work [24] we showed that the interference diagrams (c,d) of Fig. 1 can amount to  $\sim 25\%$  of the total 2p-2h responses. But for the separate charge channels the interference influence can be truly different, as we show in Fig. 3. While the interference for pp emission produces a reduction of 20%, for np emission

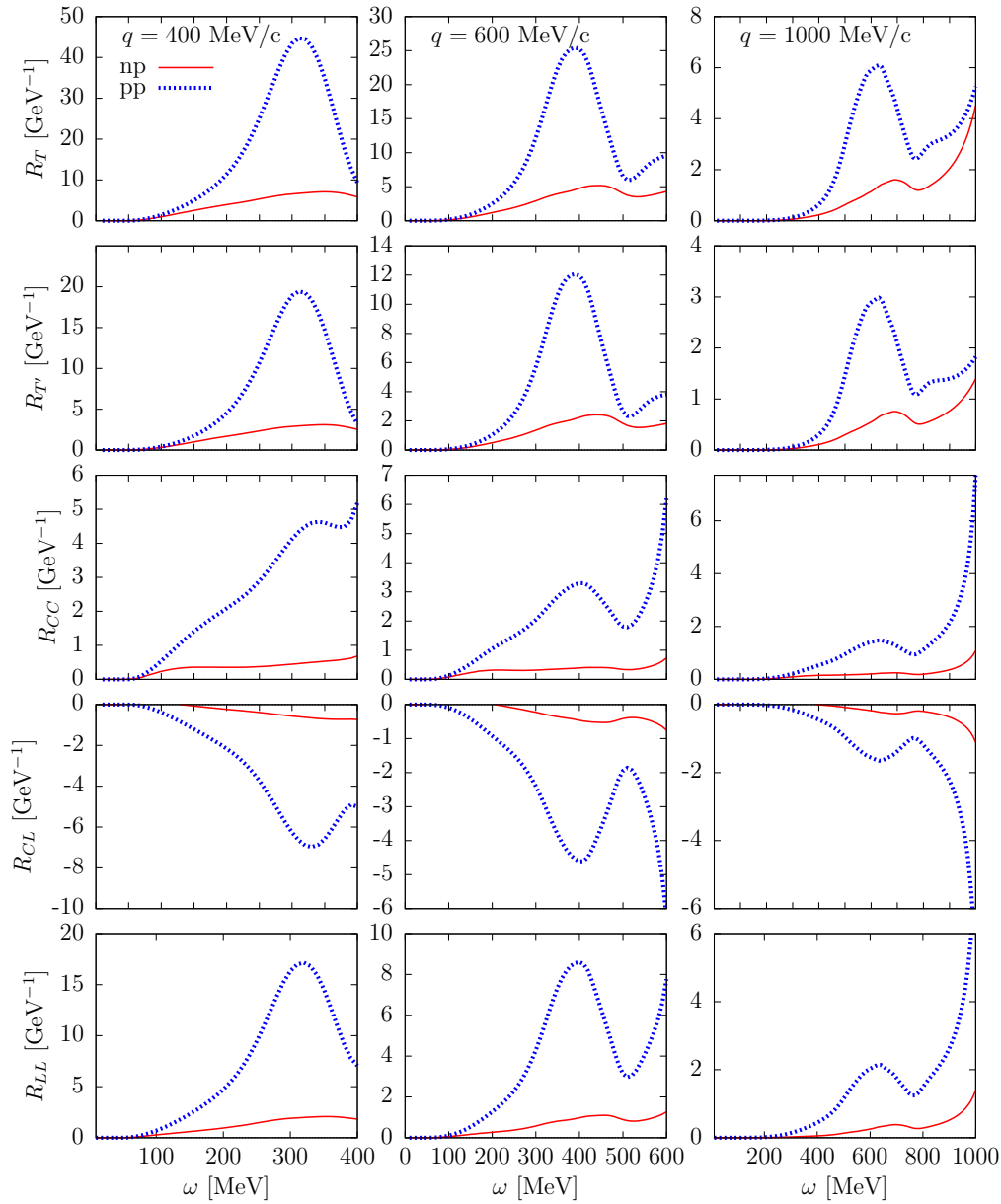


FIG. 2: (Color online) Separate pp and np 2p-2h response functions of  $^{12}\text{C}$  for three values of the momentum transfer. In all the figures the charge labels refer to the final pair of nucleons.

the reduction factor is about 1/2. Thus the ratio pp/np critically depends on the treatment on the interference contributions. The same conclusion was found for the electron scattering responses in [19]. The effect from the interference contribution is of the same size for the  $T'$  response, as shown in the lower panel of Fig. 3.

In Fig. 4 we compare the separate np and pp contributions to the response functions  $R_T$ ,  $R_{T'}$ ,  $R_{CC}$ , in the full range of momentum transfer from  $q = 100$  to  $2000$  MeV/c. This corresponds to the typical kinematic range of the neutrino experiments operating in the few-GeV region. The  $T$  response is more than twice the  $T'$  both for np and for pp channels. This seems to indicate

that the axial MEC contribution is larger than the vector one. Indeed, this can be truly observed in Fig. 5, where only the axial MEC current is included in the calculation. Note that the  $CC$  response is much smaller than the other two, except for the  $q = \omega$  point, where the  $C$  and  $L$  contributions are approximately cancelled. They would be exactly cancelled if the total current was conserved. As a matter of fact, near the photon point the seagull current dominates the MEC for high  $q$  when the  $\Delta$  resonance is far away. The axial seagull contribution is mainly longitudinal. That is why the  $CC$  response in Fig. 4 is large at the photon point for high  $q$  and the  $T$  response in Fig. 5 is so small.

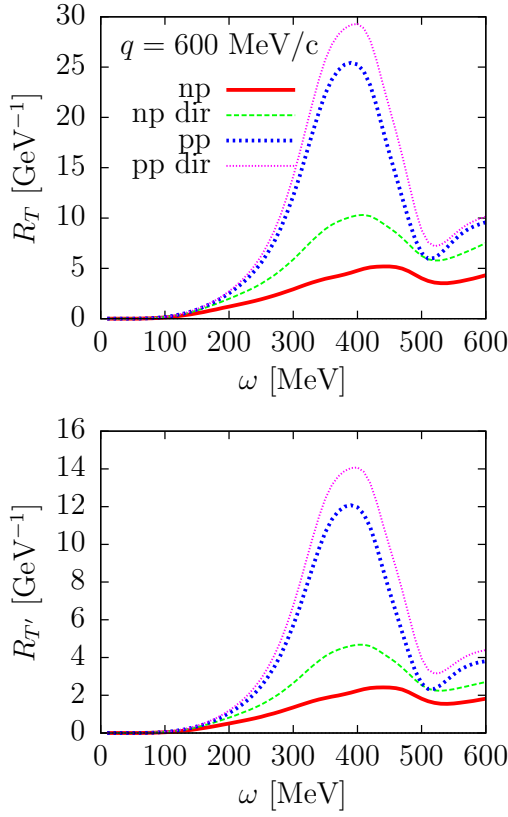


FIG. 3: (Color online) Separate pp and np contributions to the  $T$  and  $T'$  2p-2h response functions of  $^{12}\text{C}$ , for  $q = 600$  MeV/c, compared to the direct contributions obtained by neglecting the direct-exchange interferences.

To appreciate the size of the MEC 2p-2h contribution, in Fig. 6 we plot the double differential neutrino cross section per neutron,  $d^2\sigma/d\cos\theta_\mu/dT_\mu/N$ , of  $^{12}\text{C}$ , as a function of the muon kinetic energy, for  $\cos\theta_\mu = 0.85$  and for three values of the incident neutrino energy. We show the separate contributions of 1p-1h and 2p-2h channels in the RFG. The relative contribution of 2p-2h increases with the neutrino energy, and the MEC and quasielastic peaks get closer. Here the neutrino energy is fixed, while in the experiments the neutrino energy is not fixed and the flux produces an average of all the contributions around the mean energy. For typical peak energies of 1 GeV, the results of Fig. 6 indicate that one can expect a contribution of roughly 20% to the cross section from 2p-2h.

The separate pp and np channels in the differential neutrino cross section are shown in Fig. 7 for the same kinematics. The pp channel clearly dominates the 2p-2h cross section. The pp/np ratio is around 5-6 near the maximum, but its precise value depends on the kinematics. Note that the np distribution is shifted towards higher muon energies compared with the pp case. This effect can be further observed in Fig. 8, where we show the  $(\cos\theta_\mu, T_\mu)$  dependence of the 2p-2h double differen-

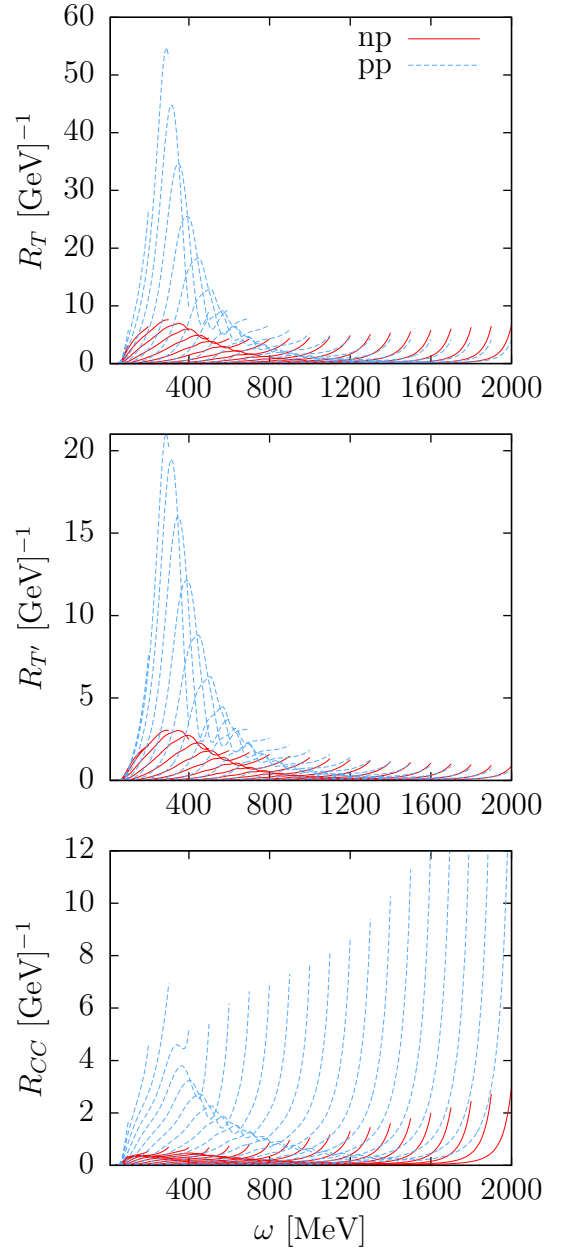


FIG. 4: (Color online) Comparison of the separate pp and np contributions to the  $T$ ,  $T'$  and  $CC$  2p-2h response functions of  $^{12}\text{C}$ , for  $q = 100, 200, \dots, 2000$  MeV/c.

tial cross section, for  $E_\nu = 1$  GeV. Indeed the second and third panels show the separate pp and np distributions. The np is much smaller than the pp one, and it is clearly shifted towards higher  $T_\mu$  and smaller angles. It can be seen that for this neutrino energy, the absolute maximum of the cross section is located around  $\cos\theta_\mu \sim 0.85$  and  $T_\mu \sim 600$  MeV, and corresponds approximately to the maximum shown in the middle panel of Fig. 7. The 2p-2h strength is concentrated in the top-right corner of Fig. 8 corresponding to small angles and large muon kinetic energies, meaning low energy transfer, around  $\omega = 300$



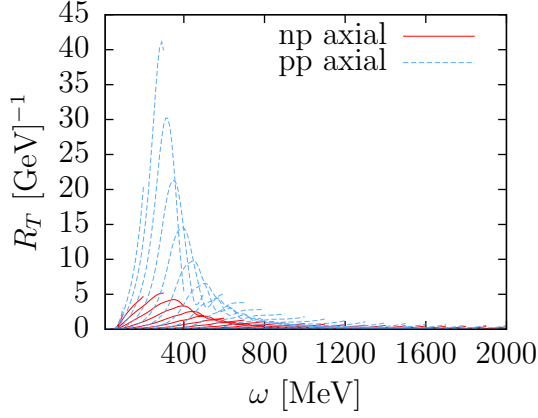


FIG. 5: (Color online) Comparison of the separate pp and np contributions to the  $T$  2p-2h response function of  $^{12}\text{C}$ , for  $q = 100, 200, \dots, 2000$  MeV/c, including only the axial MEC.

MeV. This corresponds to the excitation energy of the  $\Delta(1232)$ , which gives the main contribution to the MEC. Our calculation predicts that, when the lepton scattering angle increases, two particle emission implies a decrease of the kinetic energy of the muon or larger  $\omega$ .

#### IV. CONCLUSIONS

In this work we have studied the separate charge channels ( $\nu_\mu, \mu^- pp$ ) and ( $\nu_\mu, \mu^- np$ ), from  $^{12}\text{C}$ , integrated over the two emitted nucleons, that contribute to the 2p-2h cross section in quasielastic-like CC neutrino scattering. We have computed the response functions and double differential cross sections for several kinematics. The pp channel dominates over the np contribution in the whole domain. The pp/np ratio is about 5-6 for a wide range of neutrino energies. Future plans are to fold the cross section with the neutrino fluxes for the various neutrino oscillation experiments. Having the separate isospin contributions will allow us to apply this formalism to asymmetric nuclei  $N \neq Z$ . This will be of interest for neutrino experiments based, for instance, on  $^{40}\text{Ar}$ ,  $^{56}\text{Fe}$  or  $^{208}\text{Pb}$ .

#### Acknowledgments

This work was supported by Spanish Direccin General de Investigacion Cientifica y Tecnica and FEDER funds (grants No. FIS2014-59386-P and No. FIS2014-53448-C2-1), by the Agencia de Innovacion y Desarrollo de Andalucia (grants No. FQM225, FQM160), by INFN under project MANYBODY, and part (TWD) by U.S. Department of Energy under cooperative agreement DE-FC02-94ER40818. IRS acknowledges support from a Juan de la Cierva fellowship from Spanish MINECO. GDM acknowledges support from a Junta de Andalucia fellowship

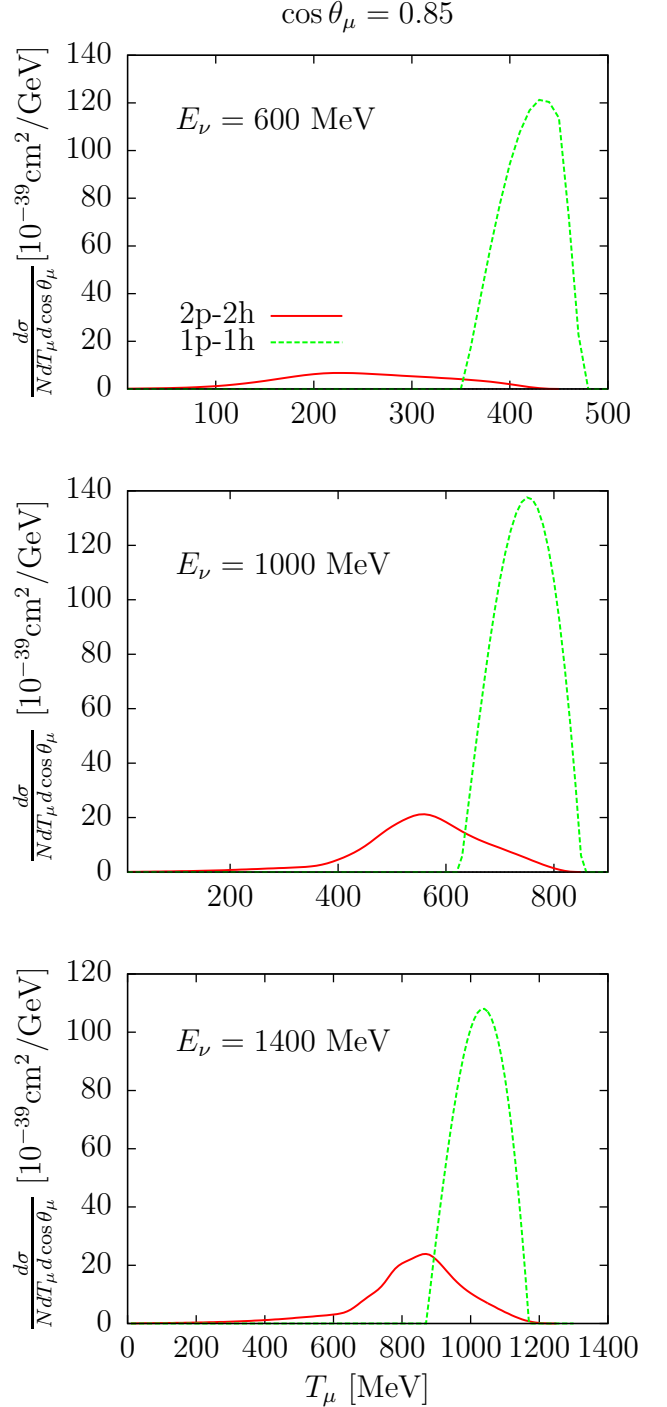


FIG. 6: (Color online) Double differential neutrino cross section per neutron of  $^{12}\text{C}$ , for fixed muon scattering angle and for three neutrino energies, as a function of the muon kinetic energy. The separate 1p-1h and 2p-2h cross sections are displayed for comparison.

(FQM7632, Proyectos de Excelencia 2011).

- 
- [1] A.A. Aguilar-Arevalo *et al.* (MiniBooNE Collaboration), Phys. Rev. **D81** (2010) 092005.
  - [2] Y. Nakajima *et al.* (SciBooNE Collaboration), Phys. Rev. **D83** (2011) 012005.
  - [3] C. Anderson *et al.* (ArgoNeuT Collaboration), Phys. Rev. Lett. **108** (2012) 161802.
  - [4] K. Abe *et al.* (T2K Collaboration), Phys. Rev. **D87** (2013) 092003.
  - [5] G.A. Fiorentini *et al.* (MINERvA Collaboration), Phys. Rev. Lett. **111** (2013) 022502.
  - [6] K. Abe *et al.* (T2K Collaboration), Phys. Rev. **D90** (2014) 052010.
  - [7] T. Walton *et al.* (MINERvA Collaboration), Phys. Rev. **D91** (2015) 7, 071301.
  - [8] P.A. Rodrigues *et al.* (MINERvA Collaboration), Phys. Rev. Lett. **116** (2016) 071802.
  - [9] R. Acciarri, *et al.*, Phys. Rev. D **90**, 012008 (2014).
  - [10] F. Cavanna, O. Palamara, R. Schiavilla, M. Soderberg and R. B. Wiringa, arXiv:1501.01983 [nucl-ex].
  - [11] L.B. Weinstein, O. Hen, E. Piasetzky, arXiv:1604.02482 [hep-ex].
  - [12] K. Niewczas, and J. Sobczyk, Phys. Rev. C **93**, 035502 (2016).
  - [13] R. Shneor, *et al.*, (JLab Hall A Collaboration), Phys. Rev. Lett. **99**, 072501 (2007).
  - [14] R. Subedi, *et al.*, Science **320** (2008), 1476.
  - [15] J. Ryckebusch, M. Vanhalst, W. Cosyn, J. Phys. G: Nucl. Part. Phys. **42** (2015) 055104.
  - [16] C. Colle, W. Cosyn, J. Ryckebusch, Phys. Rev. C **93**, 034608 (2016)
  - [17] R. Schiavilla, R.B. Wiringa, S.C. Pieper, J. Carlson, Phys. Rev. Lett. **98**, 132501 (2007).
  - [18] R.B. Wiringa, R. Schiavilla, S.C. Pieper, J. Carlson, Phys. Rev. C **89**, 024305 (2014).
  - [19] I. R. Simo, J. E. Amaro, M. B. Barbaro, A. De Pace, J. A. Caballero, G. D. Megias, and T. W. Donnelly, arXiv:1606.06480 [nucl-th]
  - [20] C. Andreopoulos, *et al.*, Nucl. Instrum. Methods Phys. Res., Sect. A **614**, 87 (2010)
  - [21] J.T. Sobczyk, Phys. Rev. C **86**, 015504 (2012).
  - [22] M. Martini, M. Ericson, G. Chanfray, J. Marteau, Phys. Rev. C **80**, 065501 (2009).
  - [23] T. Van Cuyck, N. Jachowicz, R. G. Jimnez, M. Martini, V. Pandey, J. Ryckebusch and N. Van Dessel, arXiv:1606.00273 [nucl-th].
  - [24] I. R. Simo, J. E. Amaro, M. B. Barbaro, A. De Pace, J. A. Caballero and T. W. Donnelly, arXiv:1604.08423 [nucl-th].
  - [25] A. De Pace, M. Nardi, W.M. Alberico, T.W. Donnelly and A. Molinari, Nucl. Phys. **A726** (2003) 303.
  - [26] G. D. Megias, J. E. Amaro, M. B. Barbaro, J. A. Caballero and T. W. Donnelly, Phys. Rev. D **94**, 013012 (2016).
  - [27] G. D. Megias, J. E. Amaro, M. B. Barbaro, J. A. Caballero, T. W. Donnelly and I. R. Simo, to be published.
  - [28] E. Hernandez, J. Nieves and M. Valverde, Phys. Rev. **D76** (2007) 033005.
  - [29] J.E. Amaro, M.B. Barbaro, J.A. Caballero, T.W. Donnelly and C. Maieron, Phys. Rev. **C71** (2005) 065501.
  - [30] J.E. Amaro, and E. Ruiz Arriola, Phys. Rev. D **93**, 053002 (2016).
  - [31] I. Ruiz Simo, C. Albertus, J.E. Amaro, M.B. Barbaro, J.A. Caballero, T.W. Donnelly, Phys. Rev. **D90** (2014) 033012.
  - [32] I. Ruiz Simo, C. Albertus, J.E. Amaro, M.B. Barbaro, J.A. Caballero, T.W. Donnelly, Phys. Rev. **D90** (2014) 053010.
  - [33] J. Nieves, I. Ruiz Simo, M.J. Vicente Vacas, Phys. Rev. **C83** (2011) 045501.

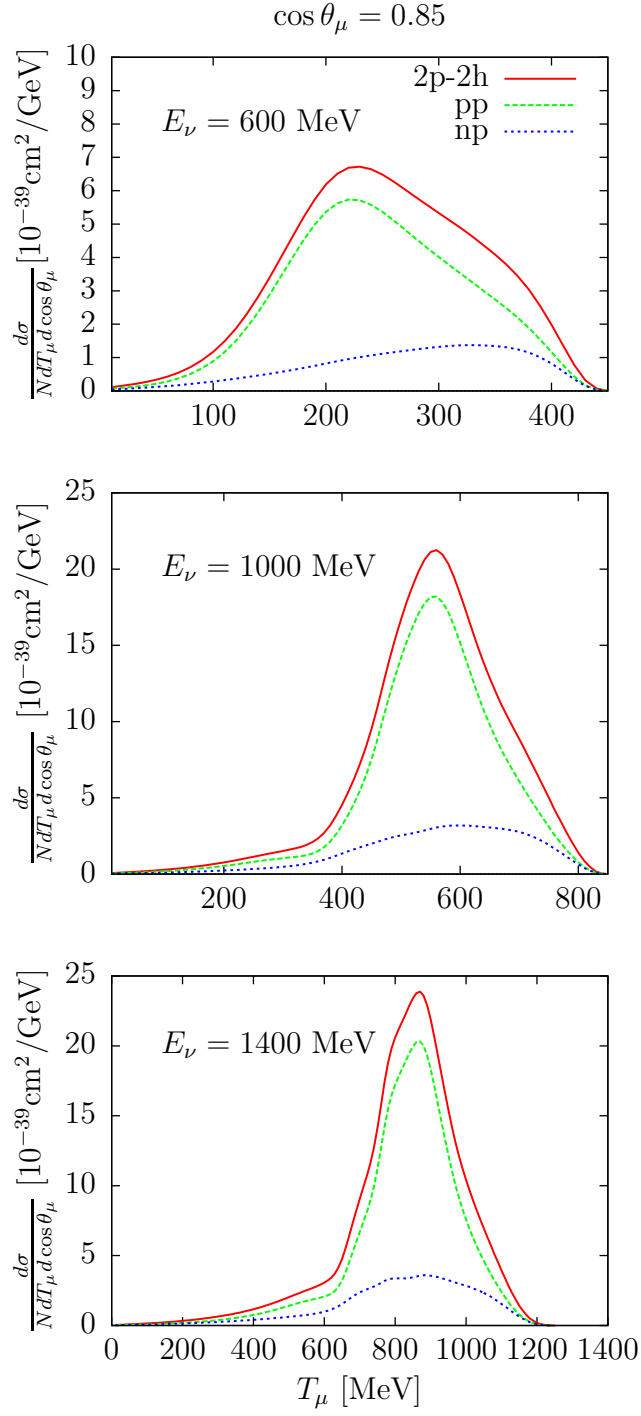


FIG. 7: (Color online) Double differential 2p-2h neutrino cross section per neutron of  $^{12}\text{C}$ , for fixed muon scattering angle and for three neutrino energies, as a function of the muon kinetic energy. The separate np and pp channels are shown.



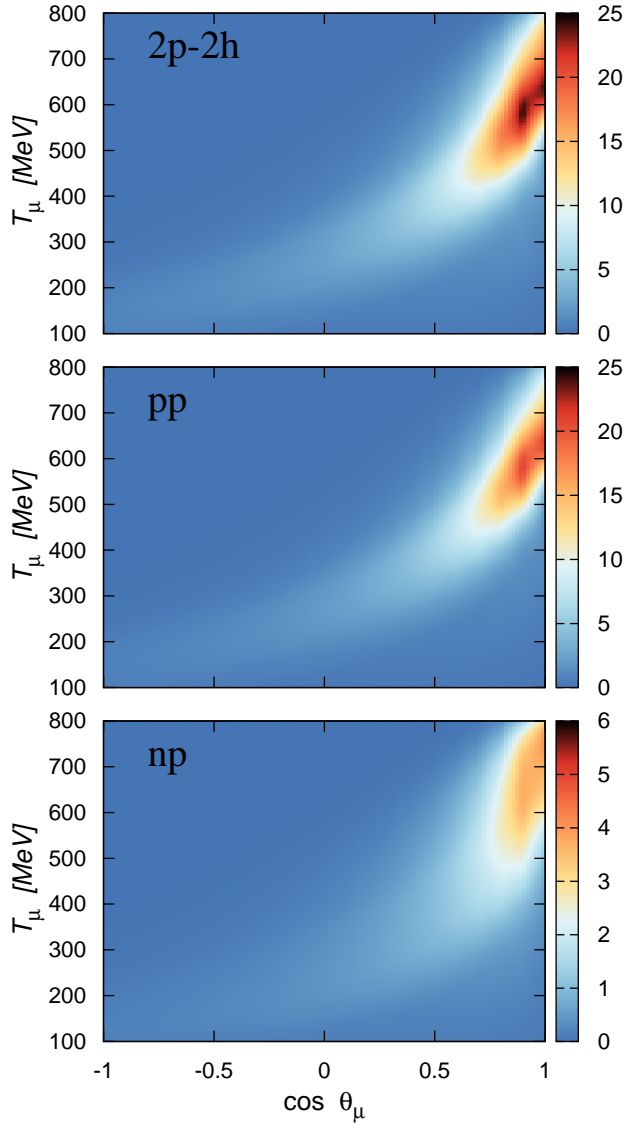


FIG. 8: (Color online) Double differential 2p-2h neutrino cross section per neutron of  $^{12}\text{C}$ ,  $d^2\sigma/d\cos\theta_\mu dT_\mu/N$ , in units of  $10^{-39}\text{cm}^2/\text{GeV}$ , as a function of  $\cos\theta_\mu, T_\mu$  for fixed neutrino energy  $E_\nu = 1$  GeV. The separate pp and np channels are shown in the middle and bottom panels, respectively.